Folding, Assembly, and Stability of the Major Light-Harvesting Complex of Higher Plants, LHCII, in the Presence of Native Lipids[†]

Dirk Reinsberg,[‡] Paula J. Booth,[§,||] Caroline Jegerschöld,[§,⊥] Bee J. Khoo,[§] and Harald Paulsen*[,‡]

Institut für Allgemeine Botanik der Johannes-Gutenberg Universität, Müllerweg 6, 55099 Mainz, Germany, and Department of Biochemistry, Imperial College of Science, Technology and Medicine, South Kensington, London SW7 2AY, UK

Received June 14, 2000; Revised Manuscript Received September 1, 2000

ABSTRACT: The influence of thylakoid lipids on the association kinetics and thermal stability of the major light-harvesting complex of photosytem II (LHCII) has been studied in vitro. The apoprotein, light-harvesting chlorophyll *a*/*b*-binding protein (Lhcb1), can be refolded and complexed with pigments in detergent solution even in the absence of lipids. Two thylakoid lipids, phosphatidyl glycerol and digalactosyl diacylglycerol, are known to interact specifically with LHCII in vivo. Here we show that both of these lipids, as well as monogalactosyl diacylglycerol, stabilize reconstituted LHCII toward thermal denaturation. Two slow kinetic phases are connected with the establishment of energy transfer between chlorophyll *b* and chlorophyll *a* and, thus, are thought to reflect the formation of the pigment−protein complex with tightly coupled chlorophylls. The lipids studied here all have the same effect on the rate of complex assembly in vitro and slow these two kinetic phases by the same degree. Both kinetic phases also slow when reactant concentrations are decreased, suggesting that the corresponding reaction step(s) involve(s) pigment binding.

Intrinsic membrane proteins are stabilized by interactions with their neighboring lipid molecules in the hydrophobic interior of the lipid bilayer. However, some membrane proteins undergo more specific interactions with lipid molecules. A plant thylakoid protein, ATP synthase, has been found to be tightly associated with sulfolipids (*1*). Photosystem II reaction center preparations are highly enriched in monogalactosyl diacylglycerol (MGDG)[1] (*2*), and further fractionation of these complexes indicates that the lipid is mostly associated with the chlorophyll (Chl) protein complexes CP43 and CP47 (*3*). The major Chl *a*/*b* light-harvesting complex of photosystem II (LHCII) contains digalactosyl diacylglycerol (DGDG) and, more tightly bound, phosphatidyl-DL-glycerol (PG) with palmitic acid or 16:1-*trans*-hexadecenoic acid as the predominant fatty acid chains (*3*, *4*).

The two lipid species bound to LHCII have differing impacts on the structure and function of the complex (*4*). DGDG is bound to isolated LHCII but can easily be washed off by detergents, leaving complexes that can no longer form 2D crystals. Their capacity to crystallize is fully restored upon readdition of DGDG, suggesting that DGDG binds in the periphery of the complex and facilitates the lateral interactions between complexes that are required for their ordered arrangement in the crystal. DGDG may have an impact on LHCII interactions with other pigment−protein complexes of the photosynthetic apparatus as well. The other lipid present in LHCII, PG, is much more tightly bound and can only be removed from the intact pigment−protein complex by the action of phospholipase or by proteolytic removal of 49 N-terminal amino acids. Both treatments cause trimeric LHCII to dissociate into monomers, suggesting that PG is specifically bound to the N-terminal hydrophilic domain of the LHCII apoprotein, light-harvesting chlorophyll *a*/*b*-binding protein (Lhcb1), and that PG stabilizes LHCII in its trimeric state. It has been suggested that PG with the unsaturated fatty acid C16:1-*trans*-hexadecenoic acid is involved in LHCII trimer stabilization (*5*−*7*). However, sodium dipalmitoyl-L-α-phosphatidyl-DL-glycerol (DPPG) is sufficient to promote lipid-dependent trimerization of recombinant LHCII reconstituted in vitro (*8*). In the N-terminal domain of LHCII apoprotein, a trimerization motif consisting of five amino acids has been identified 16 positions away from the N-terminus. Deletion of or amino acid exchanges within this motif render recombinant Lhcb1 unable to assemble into trimeric LHCII (*9*). It remains to be established whether this trimerization motif constitutes a PG binding site.

[†] This work was supported by Deutsche Forschungsgemeinschaft (PA 324/3-1,2), Deutscher Akademischer Austauschdienst, Stiftung Rheinland-Pfalz für Innovation, Fonds der Chemischen Industrie (to H.P.), The British Council, The Leverhulme Trust, and The Royal Society (to P.J.B.).

* To whom correspondence should be addressed. Phone: +49-6131-3924633; fax: +49-6131-3923787; e-mail: paulsen@mail.uni-mainz.de.

[‡] Johannes-Gutenberg Universität.

[§] Imperial College of Science, Technology and Medicine.

[||] Current address: Department of Biochemistry, University of Bristol, Bristol, BS8 1TD, UK.

[⊥] Current address: Centre for Structural Biochemistry (CSB), Karolinska Institutet, Deptartment of Biosciences, NOVUM, SE-141 57 Huddinge, Sweden.

[1] Abbreviations: Chl, chlorophyll; CMC, critical micellar concentration; DGDG, digalactosyl diacylglycerol; DOPG, sodium dioleoyl-L-α-phosphatidyl-DL-glycerol; DPPG, sodium dipalmitoyl-L-α-phosphatidyl-DL-glycerol; LHCII, light-harvesting complex of photosytem II; Lhcb1, light-harvesting chlorophyll *a*/*b*-binding protein; MGDG, monogalactosyl diacylglycerol; OG, octyl-β-D-glucopyranoside; PG, phosphatidyl-DL-glycerol; pLhcb1, precursor protein of light-harvesting chlorophyll *a*/*b*-binding protein; SDS, sodium dodecyl sulfate; TLC, thin-layer chromatography.

10.1021/bi001365z CCC: $19.00
Published on Web 10/27/2000

LHCII can be reconstituted in detergent solution by refolding its previously denatured apoprotein in the presence of Chls and carotenoids (*10*, *11*). Three distinct kinetic phases have been resolved for this in vitro assembly of LHCII so far, with time constants of the order of 10 ms, 1 min, and several minutes. These phases were monitored by a number of fluorescence signals, including intrinsic protein fluorescence, Chl *b* and Chl *a* fluorescence, as well as sensitized Chl *a* fluorescence, i.e., Chl *a* emission upon the excitation of Chl *b*. Only the slowest step, in the range of several minutes, was characterized by a decrease of Chl *b* emission and a concomitant increase of sensitized Chl *a* emission as the result of energy transfer from Chl *b* to Chl *a* and thus was interpreted as representing the formation of a functional LHCII (*12*). Recombinant Lhcb1 does not assemble in detergent solution when either Chls or carotenoids are missing (*13*). This suggests that pigment binding triggers folding of the protein.

Lipids are not required for LHCII formation in vitro, as the complex can be assembled in octyl glucoside (OG) alone. However, PG and DGDG molecules that can bind to LHCII may influence protein folding or pigment binding. Therefore, we have investigated the impact of various lipids on the folding of LHCII in mixed lipid−detergent micelles, focusing on the kinetic phase in the time range of minutes that reflects the establishment of energy transfer between the bound Chls. A preliminary report of some of these data has been presented elsewhere (*14*).

MATERIALS AND METHODS

Protein, Pigments, Lipids. Lhcb1 and its precursor protein (pLhcb1) and pigments were obtained as described previously (*12*). Chls and xanthophylls were purified from native lipids by chromatography on a silica column with hexane as the mobile phase (*15*, *16*). Absence of lipds was verified by thin-layer chromatography (TLC) (*17*). DPPG and sodium dioleoyl-L-α-phosphatidyl-DL-glycerol (DOPG) were purchased from Sigma (Munich, Germany). MGDG and DGDG were isolated from spinach and purified over TLC according to ref *18*.

Reconstitution of LHCII. The protocol of in vitro assembly of (p)Lhcb1-pigment complex was based on the experiments described by Booth and Paulsen (1996). Reconstitution was initiated by mixing equal volumes of pigment and protein solutions. The pigment solution contained 57 μM Chl *a*, 57 μM Chl *b*, 20 μM (stopped-flow experiments) or 76 μM (Fluoromax setup) xanthophylls, where the latter (corresponding to 38 μM final concentration in reconstitution mixtures) saturated the xanthophyll effect on the rate of complex assembly (see Results), 2% (w/v) OG, and 0.075% (w/v) DPPG in reconstitution buffer (100 mM sodium or lithium borate, pH 9.0, 12.5% (w/v) sucrose, and 5 mM dithioerythritol). The protein solution contained 6.2 μM protein and 0.2% (w/v) sodium dodecyl sulfate (SDS) in reconstitution buffer. Assuming a stoichiometry of 12 Chl and 3 xanthophyll molecules per apoprotein, this corresponded to a Chl−protein ratio of 1.6 and a xanthophyll−protein ratio of 1 or 4, respectively. When reconstitution was terminated, the complexes were stored at −20 °C until analysis on a partially denaturating polyarcrylamide gel (*11*). Measurements were performed with both Lhcb1 and pLhcb1. As reported before (*12*), complex formation was somewhat slower with pLhcb1. All experiments involving manually mixed components were performed with pLhcb1 because of the relatively long dead time of these kinetic measurements.

Fluorescence Measurements. Time-resolved fluorescence measurements with millisecond-time resolution were performed as described previously (*12*), using an Applied Photophysics SX.17MV stopped-flow fluorometer with a red-sensitive Hamamatsu 9828, S20 photomultiplier tube (dead-time ∼1.4 ms), at 22 °C. The path length for excitation was 2 mm; emission was measured at an angle of 90° with a path length of 2 mm. Complex assembly was initiated by stopped-flow mixing of equal volumes of the protein and pigment solutions described above. For measurements of Chl fluorescence, excitation was at 410 nm for Chl *a* and 460 or 470 nm for Chl *b* (1-nm bandwidth), and emission was detected using band-pass filters (10 nm, full width, half-maximum) centered at 650 and 670 nm (for Chl *b*) and 700 nm (for Chl *a*).

Time-resolved fluorescence measurements with a time resolution of 0.5 s were performed with a Fluoromax 2 (Jobin Yvon, Grasbrunn, Germany) fluorometer after manual mixing of pigment and protein solutions. A total of 115 μL of protein solution was added manually (by a Hamilton syringe with a peek needle) to 115 μL of pigment solution in a quartz cuvette (0.5-cm path length). The solution was mixed in the cuvette with a stirrer bar for 6 s. In contrast to the stopped-flow cuvette, manual mixing avoids any diffusion of products back into the cuvette over long time scales. A front-face setup was used in the Fluoromax to reduce reabsorption of fluorescence emission because of the high optical density of the reaction solution ($A_{660} = 2.58$ under standard conditions). With this setup, emission was detected at a 45° angle relative to the excitation beam. As a consequence of the different geometry and sensitivity of both fluorometer setups, different excitation and emission wavelengths were used. Excitation was at 470 nm, where mostly Chl *b* and only little Chl *a* is excited. Fluorescence emission was collected at 660 nm (predominantly Chl *b* emission) and 680 nm (predominantly Chl *a* emission, in this case mainly as a result of excitation of Chl *b*) simultaneously. Measurements were taken every 0.5 s for a total of 700 s. The bandwidth was 0.5 nm for excitation and 6 nm for emission. Temperature was set at 24 °C. To minimize co-excitation of Chl *a* and Chl *b*, the excitation wavelengths used in the time-resolved experiments differed slightly from the absorption maxima of both pigments (of about 435 and 455 nm, respectively, in LHCII).

Steady-state fluorescence emission spectra were measured by using the Fluoromax front-face setup with excitation (bandwidth) of 470 nm (2 nm) and emission wavelength (bandwidth) of 600 and 750 nm (2 nm), respectively.

Critical Micellar Concentration (CMC) Determination. CMC was determined by an iodine assay based on the method described by Ross et al. (*19*). Iodine dissolved in ethanol was added to detergent and mixed lipid/detergent solutions with increasing concentrations. The absorbance of micelle-solubilized iodine was measured at 360 nm.

Thermal Denaturation of Recombinant LHCII. The thermal dissociation of the assembled LHCII was determined using solutions that had been stored at −20 °C upon reconstitution measurements. Each sample (230 μL) was thawed in an

Eppendorf tube in a waterbath at 24 °C for 5 min and then immediately placed into the fluorescence cuvette thermostated at 47 °C. Measurement of sensitized Chl *a* fluorescence emission was started. Reassociation of LHCII was initiated by lowering the temperature of the fluorescence cuvette to 24 °C and the signal change was monitored. After 1400 s, a steady-state spectra was taken. Fluorometer setup including wavelengths and slit widths as well as time intervals between measurements were as given in the last section.

Data Analysis. Rate constants were determined by analyzing time-resolved data to a sum of exponential functions using TableCurve software (SPSS, Chicago, USA) or LOOK (M. Bell, Imperial College, London). Both procedures are based on a Marquardt algorithm and an iterative fitting procedure. The quality of the fits was assessed using a reduced χ^2 criterion and plots of residuals. The time constants (τ) were calculated as the reciprocals of the experimentally determined rate constants. Time constants were obtained as the average of at least three independent measurements on different samples but using the same protein preparation. Errors are quoted as standard deviation of mean.

An minor linear increase of the fluorescence signal was observed on Chl *b* and Chl *a* traces in some experiments when the pigment concentrations were 2- or 3-fold higher than standard or when solutions had aged for over 2 h prior to mixing. In the former case, this linear drift was probably caused by the deaggregation of Chls at relatively high pigment concentrations. The contribution of the linear increase never exceeded 9% of the total signal change over the entire time span of the measurement, and the drift only became obvious after much longer reaction times when both τ2 and τ3 had reached equilibrium. The linear component was subtracted from the Chl *b* trace prior to data fitting. If an additional exponential component was introduced (as opposed to the subtraction), it manifested itself as a very slow component that was quasi-linear over the time scale of measurements and had no significant effect on any faster components resolved in the fit.

RESULTS

Kinetic Data Reproducibility. LHCII assembly was initiated by mixing (p)Lhcb1 and pigments. The changes in Chl *a* and Chl *b* fluorescence were used to follow the assembly kinetics. A decrease in Chl *b* fluorescence accompanied by an increase in sensitized Chl *a* emission (i.e., after excitation of Chl *b*) reflects the establishment of energy transfer from Chl *b* to Chl *a* in newly formed pigment−protein complexes. We have previously reported that three kinetic phases accompany the folding and assembly of LHCII in OG micelles, with time constants of 10 ms, 1 min (τ1), and several minutes (τ2) (*12*). The 10-ms phase was associated with stopped-flow mixing of SDS and OG micelles. τ1 was seen as a decrease in both Chl *b* and sensitized Chl *a* fluorescence but seemed to depend on the presence of both pigments and protein, and so was assigned to the formation of a nonfunctional pigment−protein complex, which could form prior to LHCII. τ2 corresponded to the formation of functional LHCII, as seen by the loss of Chl *b* fluorescence and concomitant increase in sensitized Chl *a* fluorescence. We previously reported that the amplitude of τ2 varied up to 55% between samples. To determine the origin of this variation, the dependence of this kinetic component on the pigment−protein ratio and the age of the pigment and protein solutions (prior to mixing) have been investigated. Both factors were found to contribute to the variation in amplitude of τ2.

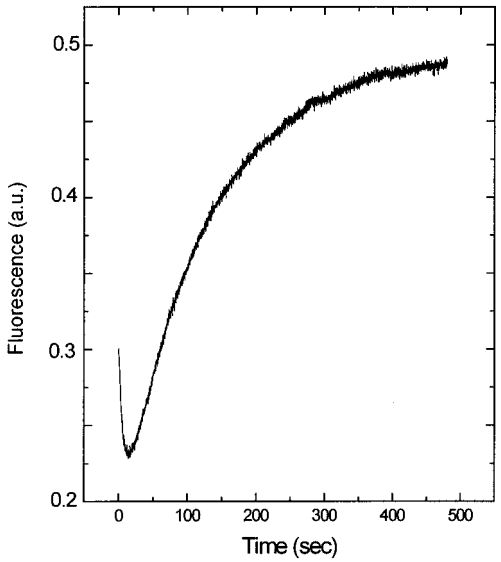

FIGURE 1: Changes of sensitized Chl *a* fluorescence (upon excitation of Chl *b*) upon mixing of the protein with pigments under standard conditions (final concentrations: 3.1 μM protein, 28.5 μM Chl *a*, 28.5 μM Chl *b*, and 10 μM xanthophyll) in a stopped-flow apparatus [excitation at 460 nm (mostly Chl *b*), emission detected at 700 nm (mostly Chl *a*)].

Figure 1 shows the changes in sensitized Chl *a* fluorescence following stopped-flow mixing of freshly prepared pigment and protein solutions (i.e., within 15 min). In addition to the 10-ms micelle mixing component, two time constants were required to fit data collected with 500 s full-scale. τ1 (decrease in fluorescence) of 7.6 ± 0.3 s and τ2 (increase in fluorescence) of 129 ± 10 s. The ratio of the amplitudes of τ1 and τ2 (i.e., A1/A2) was 0.4. Measurements over a longer time scale revealed a third slower component, τ3 (see below). The lifetimes resolved for τ1 and τ2 increased with the age of the pigment and protein solutions. For example, if these solutions were allowed to stand for 150 min before mixing τ1 was about 30 s and τ2 about 450 s with an amplitude ratio A1/A2 of 1.1. These values are similar to our earlier report where τ1 was 31 s, τ2 was 354 s, and A1/A2 was 1.25.

The time constants were also very sensitive to the pigment−protein ratio. In our earlier measurements, this ratio varied by about 20%, partly because the protein solution had frequently aged before use and begun to aggregate in the SDS solution. This has been overcome through careful monitoring of the protein concentration. Data as shown in Figure 1 were consistently obtained if the optical density of the protein in the protein solution was checked prior to mixing with the pigment solution, the protein concentration only allowed to vary within 10% and if only freshly made solutions were used (experiment starting within about 30−40 min of preparing the pigment and protein solutions).

Dependence of the Kinetics of LHCII in Vitro Assembly on Reactant Concentration. The dependence of LHCII formation on reactant concentration and detergent/lipid environment was investigated by studying the changes of

τ2 and τ3, which both reflected establishment of energy transfer and formation of functional LHCII. Most measurements were performed by manual mixing, rather than stopped-flow, to avoid back mixing artifacts over the time scales necessary to measure these relatively slow kinetics. Furthermore, it was found that both τ2 and τ3 decreased as the xanthophyll concentration was increased (Reinsberg, D., Ottmann, K., Jegerschöld, C., Booth, P. J., Paulsen, H., manuscript in preparation). This effect was saturated with the final xanthophyll concentration of 38 μM, that therefore was used to avoid any complications arising from apparent changes in xanthophyll concentration as the detergent/lipid environment was modified. Time-resolved measurements in the Fluoromax (following manual mixing of pigment and protein solutions) with this 38 μM xanthophyll concentration resulted in time constants for τ2 and τ3 of 30 and 174 s, respectively.

Figure 2 shows the changes in Chl *b* and sensitized Chl *a* fluorescence during in vitro LHCII assembly at two different reactant concentrations (manual mixing/Fluoromax setup). The protein and all pigments were used at 75% of their standard concentrations (Figure 2, panels A and B, gray trace) and twice their standard concentrations (Figure 2, panels A and B, gray trace), whereas the SDS, OG, and PG concentrations stayed the same. The kinetic traces could be fitted reasonably well with the sum of two exponentials. At the standard pigment and protein concentrations, the time constants of the two exponentials resolved for changes in Chl *b* emission (Figure 2, panel A, gray trace; τ2 and τ3 of 36 and 240 s, respectively) were within a factor of 2 or 3 of those resolved for sensitized Chl *a* emission (Figure 2, panel B, gray trace, τ2 and τ3 of 105 and 570 s, respectively). This is expected when the Chl *a* and Chl *b* signal changes in both kinetic components reflect the establishment of energy transfer. At pigment and protein concentrations of those of the standard concentrations, longer time contsants were observed in stimulated Chl *a* fluorescence (Figure 2, panel B, black trace, τ2 and τ3 of 59 and 282 s) than Chl *b* emission (Figure 2, panel A, black trace, τ2 and τ3 of 8 and 40 s, respectively). The changes in Chl *a* and Chl *b* emission still both reflect energy transfer and complex formation. However, both the Chl *a* and Chl *b* signals are complicated by a very slow, virtually linear component that reflects deaggregation of Chls at these higher concentrations (black trace in Figure 2, panel B). The sensitized Chl *a* signal was more sensitive to this deaggregation with the linear component making a substantial contribution to the fluorescence signal. All time constants reported in this paper have therefore been evaluated from the Chl *b* signal, for which the signal-to-noise was also greater than the sensitized Chl *a* signal.

When the reactant concentration was increased from 0.75- to 3-fold standard concentrations, τ2 (Figure 3, panel A) and τ3 (Figure 3, panel B) decreased from approximately 50 to an apparent 5 s and from 300 to 20 s, respectively. The apparent time constant τ2 at the highest reactant concentration, 5 s, is in the range of the dead time of the experiment and, therefore, is not included in Figure 3. The amplitude ratio A2/A3 apparently decreases with increasing reactant concentrations (Figure 3, panel C). This may be due to part of A2 being lost in the experimental dead time at higher reactant concentrations. An approximate measure for the

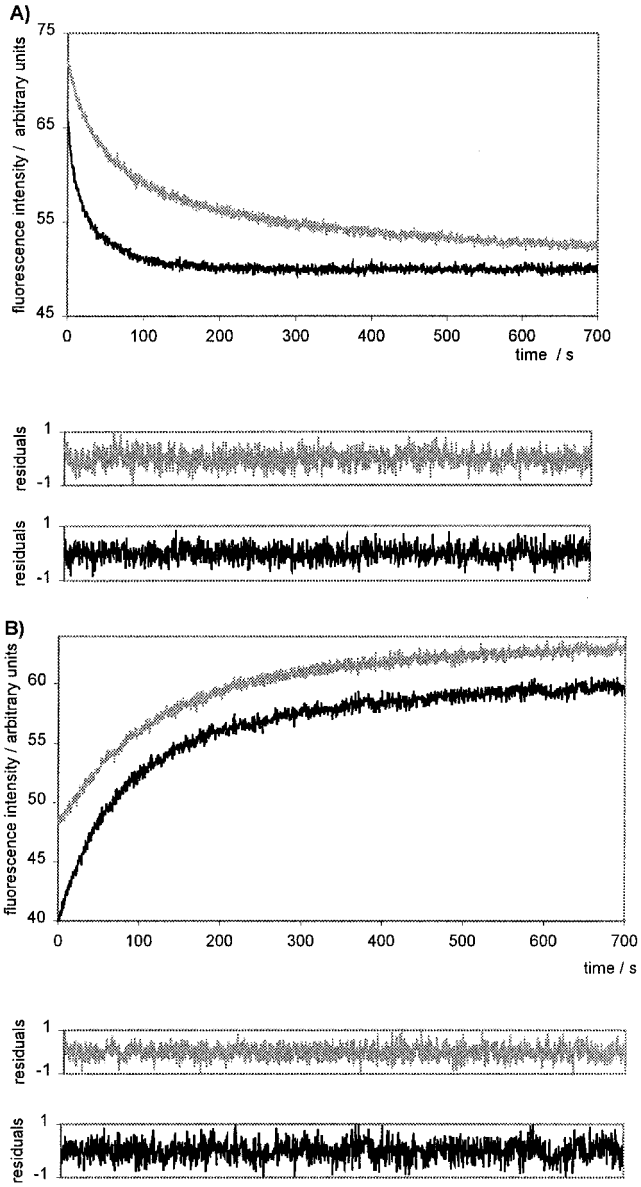

FIGURE 2: (A) Chl *b* fluorescence emission and (B) sensitized Chl *a* fluorescence upon excitation of Chl *b* during the assembly of pLhcb1−pigment complex. The gray traces show the kinetics of a reconstitution experiment using a 0.75-fold standard concentration of reactants, whereas the black traces represent the kinetics using twice the standard concentration. Residuals for a biexponential fit are shown below traces.

yield of complex formation was obtained by quantitating the quenching of Chl *b* fluorescence in the course of the experiment. In Figure 3, panel D, the Chl *b* emission measured at the end of the kinetic experiment was compared to the Chl *b* emission detected at the very beginning of the measurement. In Figure 3, panel E, the area of the Chl *b* band in the steady-state emission spectra measured upon complex formation was compared to the Chl *b* band in a control experiment lacking protein. Both measurements indicated that the extent of Chl *b* quenching, and thus the apparent yield of complex formation, did not show a trend with reactant concentrations in the range used here.

Dependence of the Kinetics of LHCII in Vitro Assembly on OG Concentration. The assembly reaction of LHCII involves mixing the protein in SDS detergent micelles with the pigments in OG micelles [which regularly contained

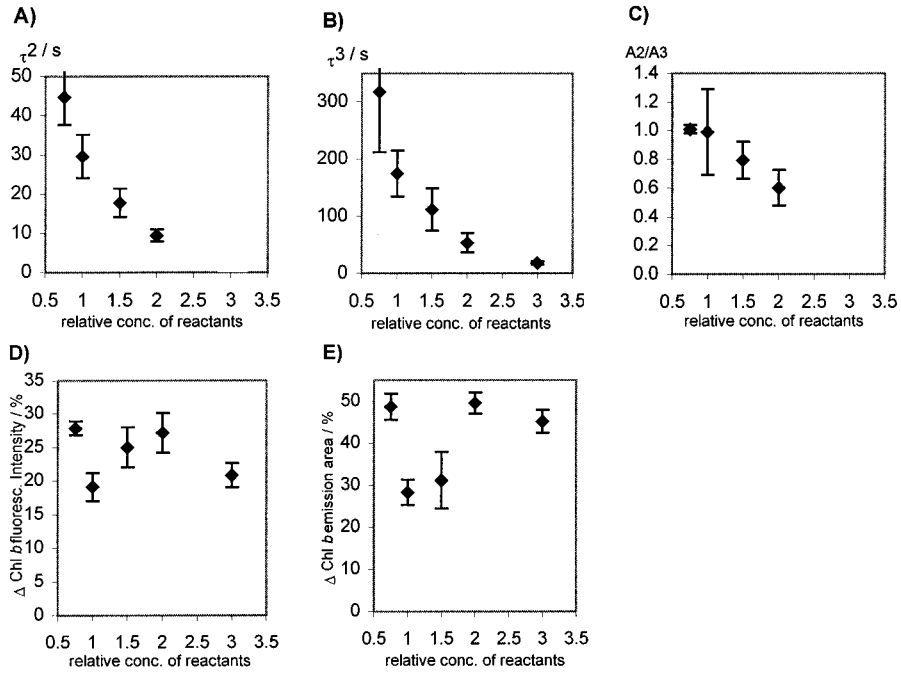

FIGURE 3: Dependence of (A) the lifetime of the faster component (τ2), (B) the lifetime of the slower component (τ3), and (C) the ratio of the amplitudes of both components (A2/A3) on the concentration of reactants (relative reactant concentrations are based on standard reactant concentrations: 57 μM Chl, 38 μM xanthophylls, and 3.1 μM protein final concentrations). Measurements were taken following manual mixing and using front-face Fluoromax setup. Time constants of less than about 10 s were derived from fewer data points because of the experimental dead time of 6 s and, therefore, are given in parentheses. (D) Dependence on reactant concentration of the relative decay of the Chl *b* fluorescence intensity (ΔChl *b* fluorescence intensity) as an approximate yield of complex formation in the reconstitution. The relative Chl *b* emission intensities were based on the initial Chl *b* signal. (E) Dependence of the approximate reconstitution yield, measured as the relative decrease of the area underneath the Chl *b* fluorescence emission spectra (ΔChl *b* emission area). The relative areas of the Chl *b* emission bands were based on the integrated Chl *b* emission bands in control experiments lacking protein.

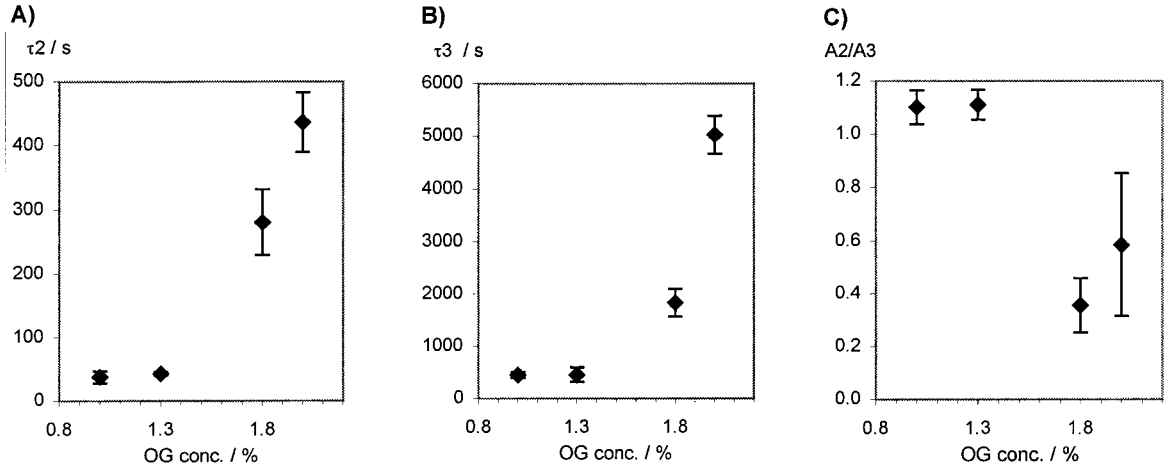

FIGURE 4: Dependence of (A) τ2 and (B) τ3 on increasing OG concentration. Standard condition is 1% (w/v) OG. (C) Ratio of the amplitudes of both components (A2/A3) with increasing OG concentration. PG was used at standard concentration [0.04% (w/v)].

0.04% (w/v) PG]. Thus, increasing the OG concentration decreases the concentration of pigments and protein in the micellar phase. Figure 4 shows that this dilution resulted in an increase of both τ2 (Figure 4, panel A) and τ3 (Figure 4, panel B) which may correspond to the dilution effect seen in Figure 3. A significant difference between these two experiments was that the apparent amplitude ratio A2/A3 decreased as τ2 and τ3 dropped because of increased reactant concentrations (Figure 3, panel C), whereas A2/A3 increased when τ2 and τ3 dropped because of a decrease in OG concentration (Figure 4, panel C). Concentrations of OG below 1% (w/v) could not be used since they did not support reconstitution of LHCII, presumably because this is close to the critical micellar concentration of OG [0.7% (w/v)], and therefore micelles might no longer form. It was also not possible to increase the SDS concentration (that would effectively have lowered the protein concentration) because a higher amount of this detergent lowered the yield of LHCII assembly under the experimental conditions used here.

Addition of Lipids to the Reconstitution Mixture Slows Down LHCII Assembly. The standard reconstitution mixture used here contained 0.04% (w/v) DPPG, corresponding to about 4.1 DPPG molecules (and 0.025 protein molecules)/OG micelle [calculated for a CMC of 0.7% (w/v) and 84 OG molecules/micelle]. Omission of DPPG did not appreciably change the time constants of complex formation

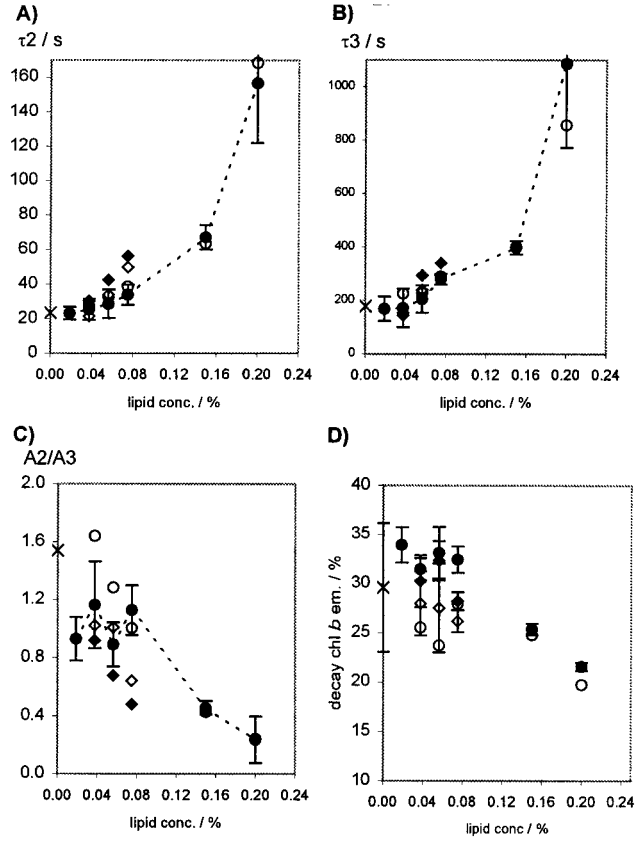

FIGURE 5: Dependence of (A) τ2, (B) τ3, and (C) the ratio of the respective amplitudes, A2/A3 on lipid concentration. (D) Dependence of the signal change in Chl *b* emission on lipid concentration. Standard deviations are only given for DPPG; deviations of other lipids are in the same range. × = 0% lipid; - -●- - = DPPG; ○ = DOPG; ◇ = DGDG; ♦ = MGDG

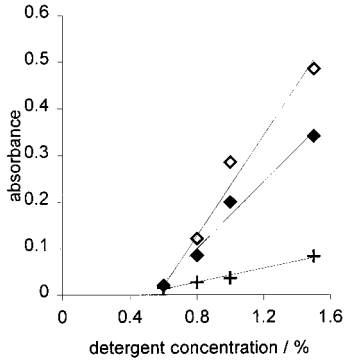

FIGURE 6: Critical micellar concentration of OG−PG mixtures depending on PG content. ◇ = OG without PG; ♦ = standard PG concentration 0.04% (w/v) PG (molar ratio of 0.015:1); + = high PG concentration 0.18% (w/v) PG (molar ratio of 0.074:1).

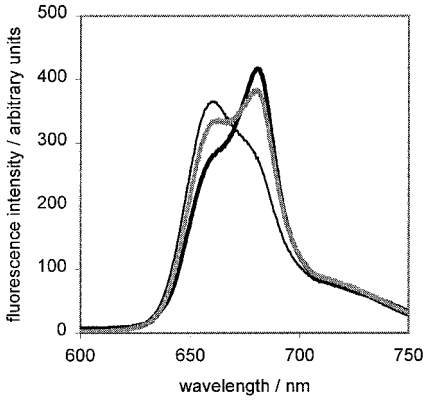

FIGURE 7: Steady-state spectra of reconstituted (black line), dissociated (thin black line, 47 °C), and reassociated (grey line, 24 °C) LHCII upon excitation of Chl *b* at 470 nm.

(Figure 5, panels A and B). However, both τ2 and τ3 became slower when the DPPG concentration was increased. At a DPPG concentration of 0.2% (w/v) (corresponding to 20 DPPG molecules/micelle), both τ2 and τ3 increased by a factor of about 8, which was accompanied by an increase in the relative amplitude of the slower phase τ3 (Figure 5, panel C). At DPPG concentrations between 0.02 and 0.04% (w/v), the two reactions contributed about equally to the total signal change (A2/A3 of about 1), whereas at a DPPG concentration of 0.2% (w/v), τ3 contributed about twice as much as τ2. Without lipids, there was a higher contribution of the amplitude of τ2 to the total signal change as compared to τ3 (A2/A3 = 1.6). Furthermore, stopped-flow measurements indicated that the amplitude of τ1 also decreased by a factor of about 5 as the DPPG concentration was increased from 0.04 to 0.15% (w/v). The relative amplitudes of the slower phases (τ2 and τ3) increased as compared to that of τ1 (*14*).

Figure 5 also shows that similar effects on the kinetics of LHCII assembly were seen when another PG lipid, DOPG (C18 chain with one unsaturated bond), was used instead of DPPG (C16 with saturated chain), or when the phospholipid was replaced with one of the two major galactolipids of the thylakoid membrane, MGDG or DGDG. Figure 5, panel D, shows the total change in Chl *b* flurorescence, based on the initial Chl *b* signal, with increasing lipid concentration, giving an approximate measure of the reaction yield as discussed above. The apparent yield remained the same over a wide range of lipid concentrations but dropped at high concentrations [0.2% (w/v) or 20 PG molecules/OG micelle].

The effect of lipids on the number and size of micelles in the lipid−detergent mixture was estimated from measuring the CMC of different OG−PG mixtures. The appearance of detergent micelles was visualized by using the absorbance at 360 nm of iodine dissolved in micelles. Figure 6 shows that the addition of 0.04 or 0.18% (w/v) PG to 1% (w/v) OG did not appreciably change the apparent CMC of about 0.6% (w/v). The different slopes seen in Figure 6 may suggest that iodine solubility in the micelles decreased with increasing PG contents.

Effect of Added Lipids on the Thermal Dissociation of Assembled LHCII. To test whether lipids have a stabilizing effect on LHCII, the thermal dissociation of the assembled complexes was investigated. Complex dissociation was reflected by an increase of Chl *b* emission and a decrease of sensitized Chl *a* emission. Figure 7 shows the steady-state fluorescence spectrum of the total reaction mixture at 24 °C (for standard reconstitution conditions) upon excitation of Chl *b* at 470 nm (thick black line). Most fluorescence arises from sensitized Chl *a* at about 680 nm while Chl *b* contributes a shoulder at about 660 nm. This demonstrates that most Chl *b* molecules are energetically coupled with Chl *a* within reconstituted complexes. Increasing the temperature to 47 °C resulted in a shift of most of the fluorescence to the 660 nm band of Chl *b* (thin black line in Figure 7), indicating that Chl *b* no longer transferred its excitation energy to Chl *a*. The shoulder still visible at 680

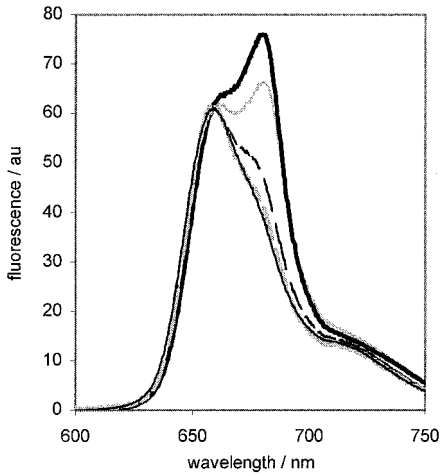

FIGURE 8: Steady-state spectra of reassociated LHCII depending on lipid added. Emission spectra were normalized at 659 nm for ease of comparison. LHCII excitation at 470 nm. Dissociated LHCII with DGDG, thin black line; LHCII under reassociation condititions in the presence of 0.08% (w/v) DGDG, thick gray dashed line; 0.08% (w/v) MGDG, dashed black line; 0.08% (w/v) DPPG, thick black line, and without lipids, thin gray line.

nm is probably due to residual energy transfer to Chl *a* in complexes that have not dissociated. When the temperature was subsequently lowered to 24 °C, a significant fraction of the initial energy transfer from Chl *b* to Chl *a* reappeared. This was seen by a decrease in the Chl *b* emission signal at 660 nm and an increase in sensitized Chl *a* fluorescence at 680 nm (grey line in Figure 7). Thus the thermal dissociation was partly reversible.

Reassociation of thermally dissociated LHCII was observed in the absence of lipids (Figure 8, thin black dashed line) and at various concentrations [between 0.02 and 0.2% (w/v)] of DPPG [Figure 8, DPPG 0.08% (w/v), thick black line]. DOPG gave the same results as DPPG (not shown). DPPG and DOPG even stimulated re-formation of LHCII, as these lipids caused a higher increase in sensitized Chl *a* emission than the one seen in the experiment without lipids. On the other hand, MGDG appeared to interfere with reassociation of recombinant LHCII. The complex still reconstituted at an MGDG concentration of 0.04% (w/v) but only small amounts of LHCII re-formed when a higher concentration of MGDG was used [0.08% (w/v), Figure 8, thick black dashed line]. DGDG inhibited the reassociation of thermally dissociated LHCII even more strongly. Only small amounts of LHCII formed in reassociation experiments with 0.04% (w/v) [Figure 8, DGDG 0.08% (w/v), gray dashed line].

The thermal stability of reconstituted LHCII was monitored by time resolving the increase in Chl *b* and decrease in sensitized Chl *a* fluorescence emission upon raising the temperature to 47 °C. The Chl *b* signal had a higher signal-to-noise ratio and was therefore used to evaluate the dissociation kinetics. LHCII that had been reconstituted in OG in the absence of lipids dissociated with a time constant of 30 s. This dissociation time constant increased to 90 and 150 s for LHCII assembled with DPPG concentrations of 0.02 and 0.2% (w/v), respectively. The lipids DOPG, MGDG, and DGDG [at concentrations of 0.04 and 0.08% (w/v)] had essentially the same effect on LHCII dissociation kinetics as DPPG (Figure 9). By contrast, an increase of the

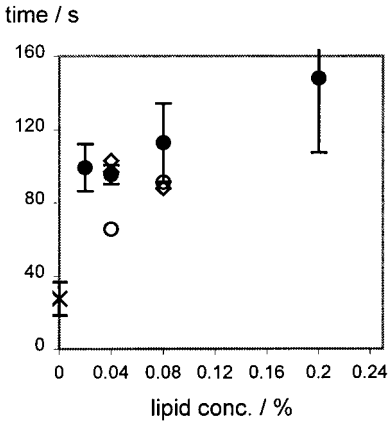

FIGURE 9: Thermal stability of LHCII as a function of lipid concentration. Time constants were obtained by monitoring the Chl *b* fluorescence increase due to dissociation of LHCII as induced by a temperature jump from 24 to 47 °C. Standard deviation of the experiments with single lipids are in the range of those with DPPG. × = 0% lipid; ● = DPPG; ○ = DOPG; ◊ = DGDG; ♦ = MGDG.

OG concentration decreased the complex stability. At an OG concentration of 1.8% (w/v), the complexes dissociated already upon thawing from −20 °C (data not shown).

DISCUSSION

Effect of Pigment−Protein Ratio and Reactant Concentration on LHCII Folding and Assembly. LHCII folding and assembly is accompanied by the establishment of efficient energy transfer between its bound Chls, which can be monitored by changes in Chl fluorescence. Formation of the folded, functional state is shown by a loss of Chl *b* fluorescence, together with an increase in sensitized Chl *a* fluorescence upon excitation of Chl *b* (Figure 1), reflecting nativelike energy transfer from Chl *b* to Chl *a*. We have shown that the folding of LHCII is very sensitive to its environment and is critically dependent upon the pigment−protein ratio and concentration. We previously reported that the increase in Chl *a* fluorescence could be represented by a single exponential with a time constant of about 300 s and a rather high variation in its amplitude of up to 55% between samples (*12*). Through careful monitoring of the protein and pigment concentrations and in particular by adjusting these two with an error of less than 10% in the reactant mixtures, we have now lowered this variability in amplitude to about 10%. Furthermore, the time constant has apparently decreased. This is due not only to the improved sample preparation and data reproducibility but also to the fact that in the earlier experiments the refolding yield decreased, because reactant solutions were kept for longer than an hour. This decrease in yield was accompanied by a decrease in the amplitude of the sensitized Chl *a* signal, together with an increase in the corresponding time constant. The improved signal-to-noise in the current work also reveals that the folding of freshly made reactant pigment and protein solutions results in an increase in sensitized Chl *a* fluorescence that is not monoexponential but reflects at least two exponential components, $\tau 2$ and $\tau 3$. This reveals a further complexity to the folding of LHCII and establishment of energy transfer between the bound Chls.

Increasing the concentration of protein and pigments decreases the rates of both time constants, $\tau 2$ and $\tau 3$, by the

same factor (Figure 3, panels A and B). Moreover, decreasing the concentration of OG micelles, which in turn will increase the effective reactant concentration, also decreases both $\tau 2$ and $\tau 3$ (Figure 4, panels A and B). Thus, both kinetic phases involve a reaction between pigment(s) and protein. There is also an apparent increase in the amplitude of $\tau 3$ as compared to that of $\tau 2$ as the reactant concentration is increased (Figure 3, panel C). Increasing the reactant concentration, however, does not appear to have a significant effect on the apparent yield of reconstituted LHCII. This suggests that under the conditions used here the folding of LHCII is not a simple equilibrium/equilibria between SDS-denatured (p)Lhcb1, pigments, and LHCII. In such an equilibrium reaction, one would expect that higher reactant concentrations would result in a higher yield of product (LHCII). However, the optical density of the Chl solution limits the maximum pigment concentration that can be investigated. Thus the range of reactant concentrations studied may be insufficient to cause a significant shift in the equilibrium. The two slow reaction components $\tau 2$ and $\tau 3$ both represent steps in LHCII formation, as the establishment of energy transfer from Chl *b* to Chl *a* is seen during both of these steps. Moreover, they seem to involve pigment binding, as they both depend on the concentration of reactants. These slow steps may either represent two parallel or two sequential reactions. The formation of LHCII seems to involve the highly cooperative binding of numerous pigments. A single, high-order pigment binding reaction would not follow exponential kinetics; however, depending on the exact nature of the reaction, the signal-to-noise, and time scale of a measurement, it may approximate to the sum of exponential functions. Thus, for example, a bimolecular reaction that strictly follows second-order kinetics can result in experimentally observed, pseudo-unimolecular rate constants, and a third order reaction can be approximated reasonably well to the sum of two exponential components. It is also possible that the observed biexponential kinetics reported here could reflect a second-, third-, or higher-order binding step(s).

Effect of Lipids on LHCII Folding and Assembly. Lipids affect the folding of LHCII in OG solution in vitro. The native thylakoid lipids, MGDG, DGDG, DPPG, and DOPG, have essentially identical effects on LHCII folding. All the lipids individually support folding of LHCII in OG/lipid mixtures and increase the thermal stability of the folded state. However, this increased stability of the folded state does not result in an increased yield of folded LHCII in the presence of the lipid. This again implies that the folding of (p)Lhcb1 in OG/lipid mixtures is not a simple equilibrium reaction. Increasing the amount of each lipid present in the OG/lipid mixture also slows down the folding of LHCII (both $\tau 2$ and $\tau 3$) at room temperature to the same extent (Figure 5, panels A and B). That also has no effect on the yield of folded LHCII nor on the relative amplitudes of $\tau 2$ and $\tau 3$, with the exception of high concentrations of lipid [0.2% (w/v) or 20 molecules/OG micelle], where the yield appears to drop and the relative amplitude of $\tau 3$ appears to increase.

The addition of lipids to the reconstitution mixture has a similar effect on the kinetics of complex formation as increasing the OG concentration with regard to both $\tau 2$ and $\tau 3$ and their relative amplitudes (Figures 3 and 4). This suggests that the lipid effect can also, at least in part, be explained by a reduction in the effective concentration of reactants.

To give a detailed interpretation of the effect of the lipids on LHCII folding, a knowledge of the physical behavior of the lipid/OG/SDS folding mixtures is required. The phase transitions of MGDG, DGDG, and PG lipids isolated from thylakoids have been measured (*20*); however, no such information exists on the mixtures of these lipids with detergents. OG itself forms micelles in aqueous solution, with a CMC of 0.7% (w/v) and about 84 OG molecules/micelle. The lipid chains of the thylakoid lipids are roughly twice as long as that of OG so that high lipid concentrations will presumably lead to distorted, elliptical micelles that could alter the CMC. However, we found that mixtures of PG and OG also seem to form micelles with a similar CMC as compared to OG alone (Figure 6).

All the lipids investigated have a similar effect on increasing the thermal stability of the assembled LHCII. This may seem surprising considering the fact that DGDG and particularly PG but not MGDG specifically bind to native LHCII (see introduction). We conclude that the lipid effect on the stability of recombinant LHCII is likely to be due to physical differences between detergent micelles with or without lipids, rather than to specific lipid−protein interaction. Binding of DGDG and PG has been shown for trimeric LHCII, and removal of bound PG either by lipase or by proteolytic cleavage of the N-terminal domain causes trimeric LHCII to dissociate into monomers (*4*). However, we have no information as to whether monomeric LHCII binds DGDG and/or PG the same way trimeric LHCII does. Experiments to solve this question are presently underway. We will also include the native PG species containing the unsaturated fatty acid C16:1-*trans*-hexadecenoic acid which has been reported to be involved in LHCII trimer stabilization (*6*, *7*, *21*).

However, a difference in the lipids was observed on cooling the heat-denatured LHCII. Heat denaturation was reversible for the PG lipids at all concentrations and MGDG at low concentrations [0.04% (w/v) lipid or 4.2 molecules/OG micelle], although after several heating/cooling cycles the yield of LHCII dropped, probably because of chemical damage to the dissociated pigments. However, with DGDG or high concentrations of MGDG, the heat denaturation was irreversible.

The different impact on reassociation of LHCII of DPPG and DOPG on one hand and DGGD and MGDG on the other hand is not likely to be due to the fatty acid components. Both DGDG and MGDG have fatty acid components predominantly C16 and C18 in length (*22*), similar to DPPG (C16) and DOPG (C18). The galactosyl lipids contain unsaturated fatty acids, mostly of the C18:3 and C16:3 types (*23*). Unsaturated fatty acids do not generally seem to inhibit complex reassociation, as we saw no difference between DPPG (C16:0 saturated) and DOPG (C18:1 unsaturated). However, it is possible that fatty acids with 3 double are responsible for the irreversibility of LHCII dissociation.

Pure MGDG is known to form a hexagonal rather than a laminar phase at room temperature. This does not explain, however, the even stronger inhibitory effect of DGDG on reassociation and, moreover, it should be kept in mind that the physical behavior of these lipids in SDS−OG−lipid mixed micelles is unknown and likely to be different from

the behavior of the pure substances. One possibility is that part of the DGDG or MGDG separated out from the mixed lipid−detergent micelles during the LHCII dissociation-association procedure, taking part of the pigments with them; this would lower the effective pigment concentration in the protein-containing micelles and, thus, impede LHCII reassociation. Light-scattering experiments may help to establish whether such a partial separation of mixed lipid−detergent micelles in fact takes place. A correlation can be noted between the size of the polar headgroup and the capacity of the lipids to promote LHCII reassociation. The lipids with the smallest headgroups, DPPG and DOPG, stimulate complex re-formation, whereas the lipid with the largest headgroup (DGDG) inhibits it. Clearly, more needs to be known about the physical behavior of mixed detergent−lipid micelles before we can explain the different impact of lipid species on the reassociation of thermally dissociated LHCII.

ACKNOWLEDGMENT

We thank David Klug and Richard Templer for helpful discussions, Ruth Horn for her help with some of the experiments, and Peter Beutelmann for providing native lipids.

REFERENCES

1. Pick, U., Gounaris, K., and Barber, J. (1987) *Plant Physiol. 85*, 194−198.
2. Murata, N., Fujimura, Y., and Higashi, S. (1990) *Biochim. Biophys. Acta 1019*, 261−268.
3. Trémolières, A., Dainese, P., and Bassi, R. (1994) *Eur. J. Biochem. 221*, 721−730.
4. Nussberger, S., Dörr, K., Wang, D. N., and Kühlbrandt, W. (1993) *J. Mol. Biol. 234*, 347−356.
5. Trémolières, A., Roche, O., Dubertret, G., Guyon, D., and Garnier, J. (1991) *Biochim. Biophys. Acta 1059*, 286−292.
6. Krupa, Z., Williams, J. P., Khan, M. U., and Huner, N. P. A. (1992) *Plant Physiol. 100*, 931−938.
7. Dubertret, G., Mirshahi, A., Mirshahi, M., Gerardhirne, C., and Trémolières, A. (1994) *Eur. J. Biochem. 226*, 473−482.
8. Hobe, S., Prytulla, S., Kühlbrandt, W., and Paulsen, H. (1994) *EMBO J. 13*, 3423−3429.
9. Hobe, S., Förster, R., Klingler, J., and Paulsen, H. (1995) *Biochemistry 34*, 10224−10228.
10. Plumley, F. G., and Schmidt, G. W. (1987) *Proc. Natl. Acad. Sci. U.S.A. 84*, 146−150.
11. Paulsen, H., Rümler, U., and Rüdiger, W. (1990) *Planta 181*, 204−211.
12. Booth, P. J., and Paulsen, H. (1996) *Biochemistry 35*, 5103−5108.
13. Paulsen, H., Finkenzeller, B., and Kühlein, N. (1993) *Eur. J. Biochem. 215*, 809−816.
14. Jegerschöld, C., Petrovic, A., Khoo, B. J., Reinsberg, D., Paulsen, H., and Booth, P. (1998) in *Photosynthesis: Mechanism and Effects* (Garab, G., Ed.) Vol. I, pp 365−368, Kluwer Academic Publishers, The Netherlands.
15. Anderson, W. H., Hawkins, J. M., Gellermann, J. L., and Schlenk, H. (1974) *J. Hattori Bot. Lab. 39*, 99−103.
16. Gellerman, J. L., Anderson, W. H., Richardson, D. G., and Schlenk, H. (1975) *Biochim. Biophys. Acta 388*, 277−290.
17. Kohn, G., Hartmann, E., Stymne, S., and Beutelmann, P. (1994) *J. Plant Physiol. 144*, 265−271.
18. Kates, M. (1986) in *Techniques of Lipidology. Isolation, Analysis and Identification of Lipids*, Elsevier, Amsterdam.
19. Ross, S. and Olivier, J. P. (1959) *J. Phys. Chem. 63*, 1671−1674.
20. Williams, W. P. (1998) in *Lipids in Photosynthesis: Structure, Function and Genetics* (Siegenthaler, P. A., and Murata, N., Eds.) pp 103−118, Kluwer Academic Publishers, Dordrecht, The Netherlands.
21. Trémolières, A. and Siegenthaler, P. A. (1998) in *Lipids in Photosynthesis: Structure, Function and Genetics* (Siegenthaler, P. A., and Murata, N., Eds.) pp 175−189, Kluwer Academic Publishers, Dordrecht, The Netherlands.
22. Murata, N. and Segenthaler, P. A. (1998) in *Lipids in Photosynthesis: Structure, Function and Genetics* (Siegenthaler, P. A., and Murata, N., Eds.) pp 1−20, Kluwer Academic Publishers, Dordrecht, The Netherlands.
23. Joyard, J., Maréchal, E., Miège, C., Block, M. A., Dorne, A. J., and Douce, R. (1998) in *Lipids in Photosynthesis: Structure, Function and Genetics* (Siegenthaler, P. A., and Murata, N., Eds.) pp 21−52, Kluwer Academic Publishers, Dordrecht, The Netherlands.

BI001365Z